

Investigating the Impact of Characteristics on Transient Power System Stability During Fault: A Case Study of Peerdawd Power Station

Jawad Hamad Hameed
Ecole Nationale d'Ingénieurs
de Gabès
Gabes University
Gabes, Tunisia
jawad20072003@gmail.com

Wssan Adnan Hashim
Medical Devices Engineering Dept.
Al-Qalam University College
Kirkuk, Iraq
wasan.eng@alqalam.edu.iq

Nabil Derbel
National Engineering School of of
Sfax, University of Sfax, Tunisia
nabil.derbel@enis.rnu.tn

Shahab Wahhab Kareem
Information System
Engineering Department
Engineering College
Erbil Polytechnic University
line 4: Erbil, Iraq
shahab.kareem@epu.edu.iq

Shadan M.J. Abdalwahd
Information System Engineering
Department
Engineering College
Erbil Polytechnic University
Erbil, Iraq
Shadan.abdalwahud@epu.edu.iq

Abstract—This study focuses on investigating the performance of the Power System Stabilizer (PSS) and the Excitation Control System during a three-phase fault with a duration of 2 seconds. Additionally, it examines the impact of different load types (light, normal, and heavy loads) on the PSS performance during transient conditions resulting from the fault. The Peerdawd Gas Power Station (PPGS) in North Iraq is used as the dynamic model for the study, incorporating the aggregated Excitation Control System (Ex2100) and the Power System Stabilizer (PSS2B). To compare the performance of the conventional power system stabilizer (CPSS) and the modern power system stabilizer (PSS2B), transient stability parameters such as damping ratio (ξ), settling time (t_s), and maximum overshoot (MP%) are analyzed. The simulation program utilizes MatlabTM/Simulink. The results of the study provide valuable insights into how load variation influences system damping based on the Power System Stabilizer (PSS).

Keywords—transient stability, damping ratio (ξ), settling time (t_s), maximum over shoot (MP%), conventional power system stabilizer (CPSS), modern power system stabilizer (PSS2B), Peerdawd Power Gas station (PPGS).

I. INTRODUCTION (HEADING 1)

An electrical power system (EPS) is a large, complex, and dynamic system that consists of various interconnected elements. Its capability to generate, transmit, and distribute electrical energy over a vast geographical area makes it susceptible to a wide range of dynamic interactions, which can affect specific components, fragments of the system, or the entire system. Power system dynamics can be categorized based on their cause, consequence, timeframe, physical character, or location in the system where they occur [1]. As the largest and most intricate man-made dynamic system, power systems require continuous monitoring and control to maintain stability. The power system is subjected to perturbations and oscillations, which can cause transitions from one operating state to another. To ensure stability, these

oscillations need to be damped. Engineers have been preoccupied with power system stability since the 1920s, however, despite significant advancements in control and protection technology, blackouts caused by instability still occur. In an effort to improve stability and control, there has been a growing trend of interconnections between regional power systems. However, the stability problem has gained new dimensions [2]. An examination of interconnected concepts is essential when studying a dynamic system. In system planning, the key concepts are system Reliability, Security, and Stability. Providing definitions of these concepts can aid in comprehending their relationships and distinctions.

System reliability refers to the likelihood of a system being able to perform a desired function under specific operating conditions throughout its lifespan. The level of reliability can be assessed based on the frequency, duration, and intensity of negative impacts on consumer service.

System Security pertains to the level of risk associated with the system's ability to endure unforeseen events without disrupting its functionality. This relates to the resilience of a system in the face of unexpected events or circumstances. Therefore, the outcome is contingent upon the current state of the system and the likelihood of a contingency event. A power system can be deemed fully reliable if it consistently maintains a state of security. Security is closely linked to the concept of robustness, which refers to the ability of the power system to withstand and recover from disturbances.

System Stability refers to the capacity of a system to maintain its normal functioning and remain stable even after experiencing a disturbance. Therefore, the outcome is contingent upon the specific operational circumstances and the characteristics of the physical disruption.

Reliability is considered the main goal in power system design and operation, based on the three aforementioned concepts. In order to achieve system reliability, it is imperative that the system remains secure for the majority of the time, both during and after periods of faults. Therefore, it

is imperative that the system remains stable. Hence, security and stability are dynamic characteristics that can be evaluated by examining the performance of the power system under specific conditions. However, reliability is assessed based on the average performance of the power system over time, and can be evaluated by observing the system's behavior over a specific duration [2], [3]. The differentiation between steady state and dynamic stability is often unclear due to the similarity of stability issues in both cases. As a result, they are typically encompassed within a single field of study. The distinction lies solely in the level of intricacy employed in the modeling of the machines. Dynamic stability analysis incorporates the inclusion of excitation systems, turbine control systems, and synchronous machine models. Steady state problems employ a straightforward generator model that considers the generator as a constant voltage source. The likelihood of dynamic instability is significantly greater than steady state instability due to the persistent occurrence of small disturbances in the power system, such as minor variations and changes in turbine speeds. These disturbances, although not substantial enough to disrupt the system's synchronism, contribute to the increased probability of dynamic instability [4], [5]. After a temporary disruption, if the power system remains stable, it will eventually return to a new state of balance with almost the entire system undamaged. The system will be restored to its normal state through the actions of automatic controls and, potentially, human operators. Conversely, if the system is not stable, it will lead to an uncontrollable situation, such as a continuous increase in the angle between generator rotors or a continuous decrease in bus voltages. Fluctuations in network conditions can cause a chain reaction of power failures, resulting in a significant portion of the power system shutting down. Through the foregoing, and according to the nature of the disturbances, the place of their occurrence and the strength of their impact on the parameters of the power system, the power system stability must be classified into (i) Rotor angle stability; (ii) Voltage stability; and (iii) Frequency stability as shown in Figure 1 below [1], [2], [5], [6], [7]. In order to improve the stability of the power system, it is suggested to install a straightforward and efficient supplementary excitation controller in this system. PSS devices and supplementary controllers were employed in a power system to maintain a reliable balance between demand and generation, ensuring high power quality [8], [9].

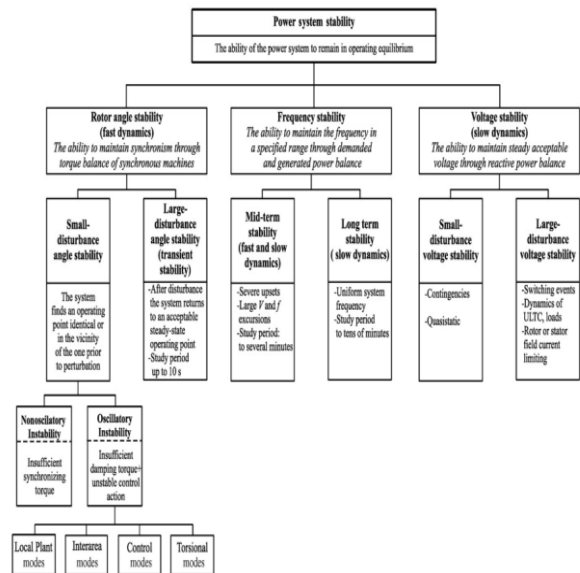


Fig. 1. Power system stability classification.

During the Transient stability, such as a fault on a transmission line or a sudden change in load the generators may experience significant swings in their rotor angles, and it is crucial for the system to regain stability and return to a synchronized state.

The damping ratio (ζ) and natural frequency (ω_n) play essential roles in determining the transient stability of a power system:

1. **Damping Ratio (ζ):** In the context of power systems, the damping ratio indicates how quickly the oscillations in the system decay. It is influenced by various factors, including generator and transmission line parameters, excitation and governor systems, and control strategies. Effect on Transient Stability: Higher damping ratios lead to faster decay of oscillations, resulting in better transient stability. If the damping ratio is low, the system can exhibit sustained oscillations, leading to instability and potential cascading failures.
2. **Natural Frequency (ω_n):** The natural frequency represents the inherent oscillation frequency of the system. It depends on the system's inertia and stiffness characteristics. Effect on Transient Stability: A higher natural frequency can improve transient stability. When the natural frequency is high, the system's inherent tendency to oscillate quickly can help it recover from disturbances and maintain synchronization. However, excessively high natural frequencies can lead to increased stresses on equipment and may require more stringent control measures.

To ensure good transient stability in a power system, engineers need to design and implement control strategies that optimize the damping ratio and natural frequency. Various methods, such as power system stabilizers (PSS), excitation control, and governor response adjustments, are used to enhance damping and increase the natural frequency [10], [11], [12]. In [13], a two-degree of freedom PID

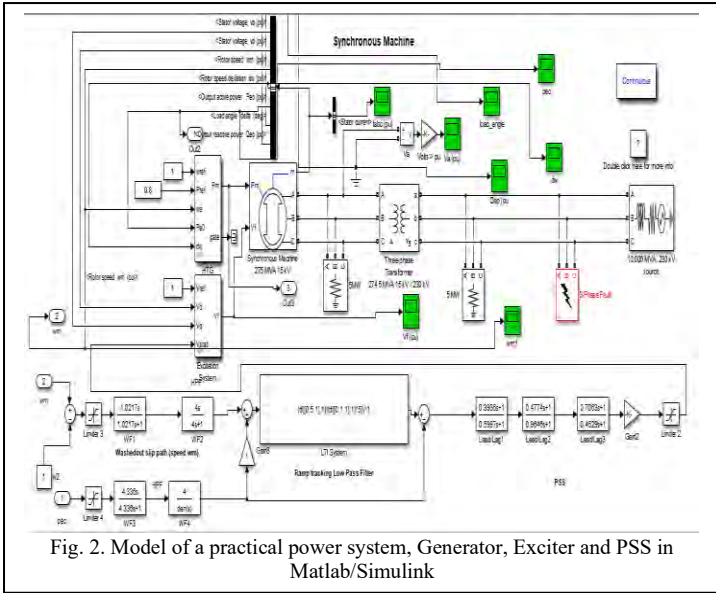


Fig. 2. Model of a practical power system, Generator, Exciter and PSS in Matlab/Simulink

stabilizer is designed to improve the damping of the system by tuning the stabilizer parameters using particle swarm optimization (PSO). The goal of [14] is to examine the impact of PSS-based PID controllers on the damping of electromechanical oscillations in power systems. A comparative analysis of three distinct power system stabilizers (CPSS, PIPSS, and PID-PSS) has been conducted on a Single Machine Infinite Bus (SMIB) power system under three different operating conditions (normal load, heavy load, and light load). This paper focuses on a real case study of the Peerdawod Gas power station, which is situated in the southern region of Iraq, specifically in Erbil. The block diagram model of the power station is depicted in Figure 2. We analyzed the transient stability state under three distinct load conditions: light load, normal load, and heavy load. By implementing two distinct types of power system stabilizers. The conventional Power System Stabilizer (CPSS) only has one input, which is the active power. In contrast to its predecessor, the modern Power System Stabilizer (PSS2B) features a more advanced design with two inputs. These inputs include the active power input (P_e) and the rotor speed deviation input ($d\omega$). This enhanced configuration allows for improved stability and control of the power system.

II. ANALYSIS OF TRANSIENT TIME RESPONSE PARAMETERS

Transient time response analysis is an important aspect of power system stability assessment. To derive the equations for the damping ratio (ζ) in the transient stability analysis of a power system, we need to consider the differential equations that govern the system's behavior during transient conditions. Specifically, we will look at the equations that describe the dynamic response of the generator rotor angle following a disturbance, which is one of the key variables in transient stability analysis. The differential equation that governs the rotor angle (δ) dynamics is given by:

$$M \frac{d^2 \delta}{dt^2} + D \frac{d\delta}{dt} + K\delta = P_m - P_e \quad (1)$$

where:

M is the moment of inertia of the generator rotor.

D is the damping coefficient.

K is the stiffness coefficient.

P_m is the mechanical power input to the generator.

P_e is the electrical power output from the generator.

During transient stability analysis, the assumption is made that the system is operating close to its steady-state condition before the disturbance. Therefore, we can consider the deviations from the steady-state as small, leading to a linearized form of the above equation.

Let's assume

$$\delta = \delta_s + \Delta\delta \quad (2)$$

where:

δ_s is the steady-state rotor angle.

$\Delta\delta$ is the small deviation from the steady-state.

Now, we can substitute this into the differential equation and keep only the linear terms in the deviation:

$$M \frac{d^2(\delta_s + \Delta\delta)}{dt^2} + D \frac{d(\delta_s + \Delta\delta)}{dt} + K(\delta_s + \Delta\delta) = P_m - P_e \quad (3)$$

Since the system is operating at steady-state before the disturbance, we have ($P_m = P_e$). Neglecting the higher-order terms, we can rewrite the equation as:

$$M \frac{d^2 \Delta\delta}{dt^2} + D \frac{d\Delta\delta}{dt} + K\Delta\delta = 0 \quad (4)$$

Next, we can express this equation in a standard second-order linear form:

$$\frac{d^2 \Delta\delta}{dt^2} + \frac{D}{M} \frac{d\Delta\delta}{dt} + \frac{K}{M} \Delta\delta = 0 \quad (5)$$

Comparing this with the standard second-order linear control system differential equation:

$$\frac{d^2 x(t)}{dt^2} + 2\zeta\omega_n \frac{dx(t)}{dt} + \omega_n^2 x(t) = 0 \quad (6)$$

$$G(s) = \frac{\omega_n^2}{s^2 + 2\zeta\omega_n s + \omega_n^2} \quad (7)$$

$$\zeta = \frac{D}{2\sqrt{KM}} \quad (8)$$

$$\omega_n = \sqrt{\frac{K}{M}} \quad (9)$$

where:

- $x(t)$ is the state variable (e.g., generator rotor angle or voltage deviation),
- ζ is the damping ratio (dimensionless),
- ω_n is the natural frequency (rad/s),
- s is the complex frequency variable.

The above equation is a standard form of a second-order linear differential equation, and it represents the behavior of a power system after a disturbance, such as a fault or sudden load change. The transient time response describes how the system returns to its steady-state after the disturbance is removed [10], [12].

Damping Ratio (ζ) effect: The damping ratio is crucial in determining the stability of the power system. It is a dimensionless parameter that reflects the system's ability to dissipate energy and avoid oscillatory behavior. The damping ratio affects the system response as follows:

1. When ($\zeta = 0$) it's called undamped system, during this case the system response will be oscillatory, and the system is highly unstable. The rotor angles or voltages will oscillate without converging to a steady-state value, leading to instability.
2. When ($0 < \zeta < 1$) it's called underdamped system and the system response will be oscillatory, but the oscillations will gradually decrease in amplitude over time. Although the system may reach a steady-state eventually, it could take a significant amount of time, leading to suboptimal performance.
3. When ($\zeta = 1$) it's called critically damped system, In this case the system response reaches its steady-state in the shortest time possible without oscillations. Critically damped systems achieve stability relatively quickly but do not overshoot their steady-state values.
4. When ($\zeta > 1$) it's called overdamped system, For this case, the system response will not oscillate, but it will take longer to reach the steady-state compared to a critically damped system. Overdamped systems are stable but may have slower response times [10], [11].

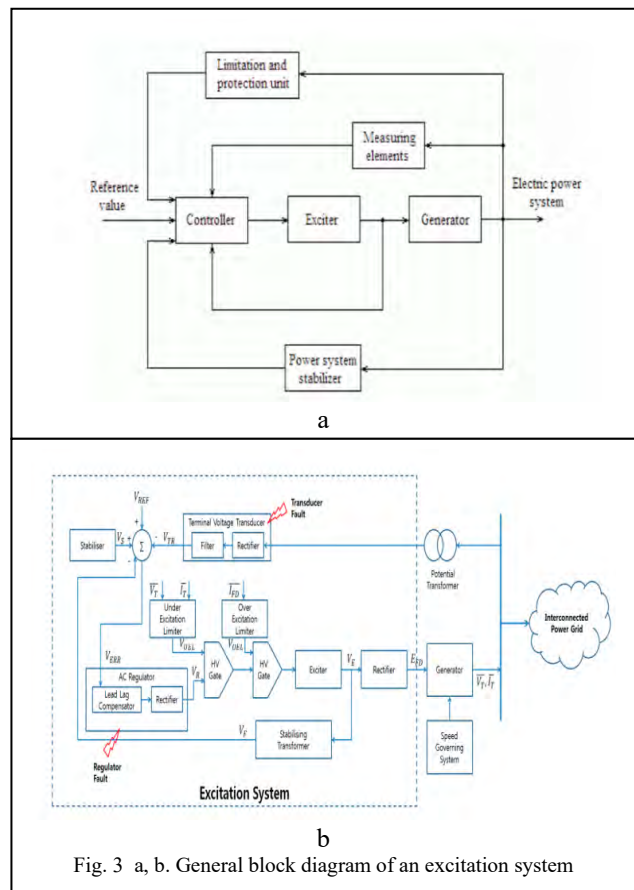
In summary, a power system with a damping ratio closer to 1 (critically damped) exhibits the best stability and quickest response to disturbances, while lower or higher values of (ζ) can lead to unstable or suboptimal system behavior. Therefore, in order to achieve a satisfactory transient response in a second-order system, the damping ratio should fall within the range of (0.4 to 0.8). Values of (ζ) less than 0.4 result in an excessive overshoot in the transient response, while a system with a ζ value greater than 0.8 exhibits sluggish response [10], [11]. The natural frequency (ω_n) denotes the intrinsic frequency at which the system would oscillate in the absence of damping ($\zeta = 0$). It influences the system's response speed to disturbances. During Higher (ω_n) value, A larger natural frequency implies that the power system is more "stiff" and has a faster response to disturbances. It means the system can handle changes more quickly and effectively, which is generally desirable for power system stability. However,

excessively high (ω_n) values might lead to higher stress on the system components. In the Lower (ω_n) a smaller natural frequency indicates a less "stiff" system, leading to a slower response to disturbances. While this can provide stability, it might also result in prolonged oscillations or delayed recovery, especially if the damping ratio (ζ) is low.

Finding the right balance between (ζ) and (ω_n) is crucial for power system stability. A critically damped system ($\zeta = 1$) with an appropriate natural frequency (ω_n) generally represents a stable and well-performing power system. However, in practice, power systems are highly complex, and stability analysis involves more detailed models and considerations beyond this simplified analysis [15], [16].

III. POWER SYSTEM STATION

The Peerdawd Gas Power Station (PPGS) in northern Iraq is an essential case study in this paper. With a total power capacity of 1500 MW, the power station consists of ten units. Each unit is represented by a 2-axis nonlinear machine model (X_q and X_d). To ensure stable operation, the power station is equipped with an (EX2100) excitation system that incorporates a fully integrated digital lead/lag Power System Stabilizer (PSS2B). The (PSS2B), which follows the integral of accelerating power (P_{acc}) principle, is fully compatible with



the (EX2100) excitation system. For a visual representation of the system arrangement, refer to the Matlab/Simulink diagram shown in Figure 2.

A. Synchronous Generator Model

The Peerdawod Gas power station (PPGS) employs a Sixth-Order model to represent its synchronous generator.

$$2H\Delta\dot{\omega} = P_m - P_e \quad (10)$$

$$\dot{\delta} = \Delta\omega \quad (11)$$

$$T'_{do}\dot{V}'_q = E_f - V'_q + I_d(X'_d - X'_q) \quad (12)$$

$$T'_{qo}\dot{V}'_d = -V'_d + I_q(X'_q - X'_d) \quad (13)$$

$$T''_{do}\dot{V}''_q = V'_q - V''_q + I_d(X'_d - X''_d) \quad (14)$$

$$T''_{qo}\dot{V}''_d = V'_d - V''_d + I_q(X'_q - X''_q) \quad (15)$$

B. Excitation System

The generator excitation system is a vital component of the electric power system of a synchronous generator, as it serves as the primary source of electrical energy, as depicted in Figure 3 a,b. The primary purpose of the excitation system is to supply direct current (d.c) to the field winding of the synchronous machine. Furthermore, it carries out control and protective functions that are crucial for the power system to operate effectively by regulating the field voltage and, consequently, the field current. The control functions encompass the regulation of the terminal voltage (V_T) and reactive power transmission, as well as the improvement of system stability. The excitation system measures the terminal bus voltage (V_T) and compares it to a predetermined reference voltage (V_{ref}). The Automatic Voltage Regulator (AVR) utilizes error signals to drive multiple control circuits, enabling it to determine the desired and actual signals through a comparison process. The protective functions ensure that the capability limits of the synchronous machine, excitation system and other equipment are not exceeded. Hence, the generators facilitate the conversion of mechanical energy, usually derived from turbines, into electrical energy. However, energy transformation can only occur if generator excitation is present. The generator's excitation also plays a role in determining the values of output parameters such as voltage and reactive power. Controlling the excitation of the generator directly influences the amount of energy produced by the generator, which in turn impacts the overall stability of the electric power system [17], [18], [19], [20]. The excitation system serves two primary functions:

1. The voltage regulator establishes a desired voltage value at the terminals of the generator bus during steady state.
2. The excitation control system provides supplementary reactive power to the power system during disturbance events, such as short-circuit faults, in order to sustain the voltage at the generator terminal. This enhances the synchronizing torque and allows the generator to maintain synchronism, thereby improving the transient stability of the connected system [3], [16].

The excitation system typically consists of two primary components that supply the excitation current:

1. The exciter is responsible for supplying power to the generator rotor field circuit.
2. The control component consists of the autonomic voltage regulator (AVR), measuring elements, power system stabilizer (PSS), and limitation and protection unit, as shown in Figure 3 a,b [19], [21], [22].

C. Power System Stabilizer

A Power System Stabilizer (PSS) is a feedback controller used in synchronous generators. It provides an extra stabilizing signal to the Automatic Voltage Regulator (AVR) by adjusting the voltage reference input. This helps to reduce Low Frequency Oscillations (LFO) in the system [23], [24], [25], [26]. Power System Stabilizers (PSS) are widely employed to enhance the damping of these modes. The primary objective of the Power System Stabilizer (PSS) is to mitigate the oscillation of the generator rotor within the frequency range of (0.1 to 3) Hz. This is accomplished by adjusting the excitation of the generator in a manner that generates electrical torque elements that are synchronized with the deviations in rotor speed. The Power System Stabilizer (PSS) helps enhance the stability of small signals in power systems [27], [28]. The goal is to guarantee that the Power System Stabilizer (PSS) delivers the highest level of enhanced damping for all electromechanical oscillations within the desired frequency range. Two prevalent oscillation patterns that can be easily resolved using a Power System Stabilizer (PSS) are: a) the oscillation of a lone generator or plant against the remainder of the power system, and b) the oscillation between a small number of generators in close proximity to each other [27], [29]. This paper will utilize the contemporary power system stabilizer known as (PSS2B). The system combines two input signals, namely electrical

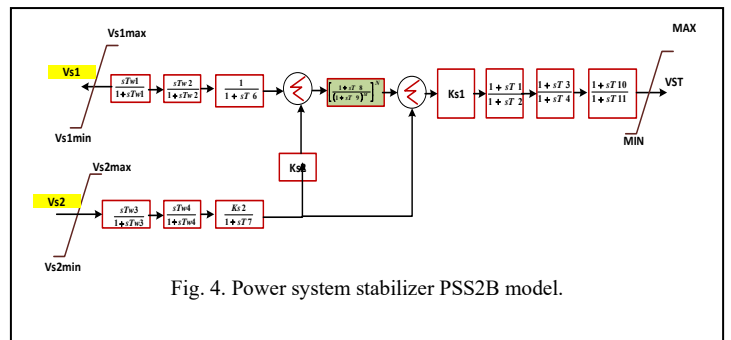


Fig. 4. Power system stabilizer PSS2B model.

power and rotor speed, to generate an equivalent speed signal that is directly proportional to the integral of accelerating power. The (PSS2B) is a crucial component of the dual input power system stabilizer, as depicted in Figure 4 [30]:

The speed deviation is equivalent to the integral of the accelerating power divided by the inertia constant ($M = 2$ H). Therefore, by assessing the speed signal, it is possible to create a stabilizer that relies on it. In the context of (PSS2B), mechanical power effects are considered to be easily

quantifiable through purely electrical signals, as demonstrated in Equations (16-21) below:

$$\Delta\omega_{eq} = \frac{1}{2H} \int (\Delta P_m - \Delta P_e) dt = \frac{1}{2H} \int P_{acc} dt \quad (16)$$

$$\Delta\omega_{eq} = \frac{1}{M} \int \Delta P_m dt - \int \Delta P_e dt = \frac{1}{M} \int P_{acc} dt \quad (17)$$

$$M\Delta\omega_{eq} = \int \Delta P_m dt - \int \Delta P_e dt = \int \Delta P_{acc} dt \quad (18)$$

$$M\Delta\omega_{eq} + \int \Delta P_e dt = \int \Delta P_m dt \quad (19)$$

$$\int \Delta P_{acc} dt = -\int \Delta P_e dt + [M\Delta\omega_{eq} + \int \Delta P_e dt] \quad (20)$$

$$\frac{\Delta P_{acc}}{MS} = -\frac{\Delta P_e(s)}{MS} + G(s) \left[\frac{\Delta P_e(s)}{MS} + \Delta\omega_{eq}(s) \right] \quad (21)$$

The variables (P_m , P_e , and P_{acc}) represent the mechanical, electrical, and accelerating powers of the generator, respectively, measured in per-unit. The variables (M and H) represent the inertia constant, measured in seconds. The variable (ω_{eq}) represents the equivalent angular speed, measured in per-unit. The variable ($G(s)$) represents the transfer function of the low-pass filter. Hence, the integration of mechanical power is directly linked to the rotational speed of the shaft and the electrical power. The (PSS2B) consists of two primary components: the filters, which include the washing filter that acts as a high pass filter for the input path involving electrical power change (ΔP_e) and speed rotor deviation ($\Delta\omega$), and the stabilizing parts, which incorporate lead lag compensation. These components are depicted in Figure 4 [29]. The input accelerating power (P_{acc}) is integrated and serves as the input for the stabilizing components, which consist of two or three lead-lag phase compensations, namely (PSS) Gain (K_{ps1}), and an output limit function (VST_{MAX} and VST_{MIN}), as depicted in Figure 5 [29].

$$G(s)_{PSS} = K_{pSS} \left[\frac{1+sT_1}{1+sT_2} * \frac{1+sT_3}{1+sT_4} * \frac{1+sT_{10}}{1+sT_{11}} \right]. \quad (22)$$

$$VST = G(s)_{PSS} * \frac{\Delta P_{acc}}{MS} \quad (23)$$

$$VST = K_{pSS} \left[\frac{1+sT_1}{1+sT_2} * \frac{1+sT_3}{1+sT_4} * \frac{1+sT_{10}}{1+sT_{11}} \right] * \frac{\Delta P_{acc}}{MS} \quad (24)$$

where :

K_{pSS} represents the proportional gain of the power system stabilizer (PSS) in per unit (pu). (T_1 , T_2 , T_3 , T_4 , T_{10} , and T_{11}) represent the time constants for the lead and lag components of the (PSS) in seconds. VST represents the output of the PSS in per unit (pu). The values of (T_1 , T_2 , and

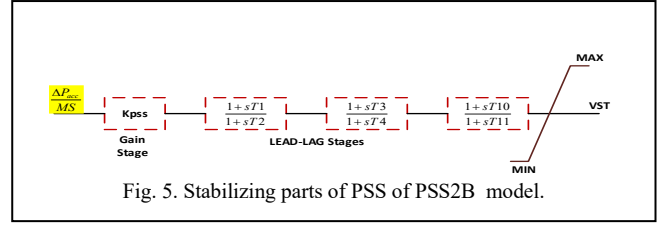


Fig. 5. Stabilizing parts of PSS of PSS2B model.

T_3) must be between (0.02 and 2), while the value of (T_4) must be between (0.02 and 6).

IV. TRANSIENT STATE RESPONSES:

MATLAB Simulink was utilized to execute the simulation of the actual case study under three different load conditions: light load at a power factor of 60%, normal load at a power factor of 80%, and heavy load at a power factor of 95%. In these instances, I will propose two alternatives:

- Conventional Power System Stabilizer (CPSS) has a single input, which is the active power.
- Modern Power System Stabilizer (PSS2B) has two inputs: the active power input (P_e) and the rotor speed deviation input ($d\omega$).

Next, the impact of the load case and the performance of the Power System Stabilizer (PSS) were observed by analyzing the response to various transient parameters such as damping ratio (ζ), maximum overshoot (%MP), settling time (t_s), peak time (t_p), natural frequency (ω_n), and damping frequency (ω_d). These parameters were measured for two power system parameters, namely voltage terminal (V_T) and rotor speed (ω_m) in per unit (pu), during a three-phase fault lasting 2 seconds. The results can be seen in Figures 6-30 and Tables (I-).

A. Transient state of PPGS during fault at light load

Tables I-III illustrate the transient parameters' values,

which include the damping ratio (ζ), maximum overshoot (%MP), un-damped natural frequency (ω_n), damped natural frequency (ω_d), peak time (t_p), terminal voltage peak (V_{TP}), and settling time (t_s). These parameters are significant in determining the terminal voltage (V_T), rotor speed (ω_m), and active power output (P_{e0}) responses with the traditional Power System Stabilizer (PSS) and the more advanced PSS (PSS2B).

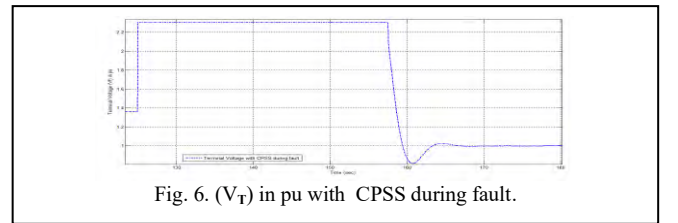


Fig. 6. (V_T) in pu with CPSS during fault.

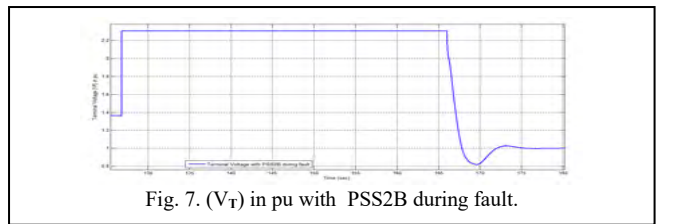


Fig. 7. (V_T) in pu with PSS2B during fault.

Analyzing the results from Tables I-III reveals a notable

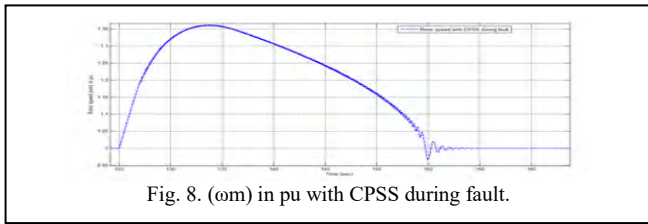


Fig. 8. (ω_m) in pu with CPSS during fault.

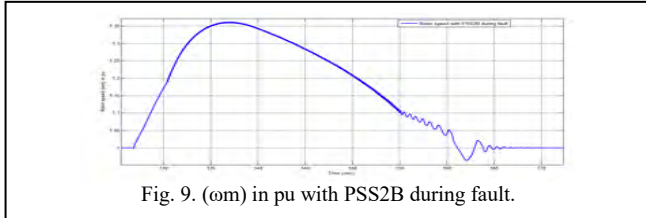


Fig. 9. (ω_m) in pu with PSS2B during fault.

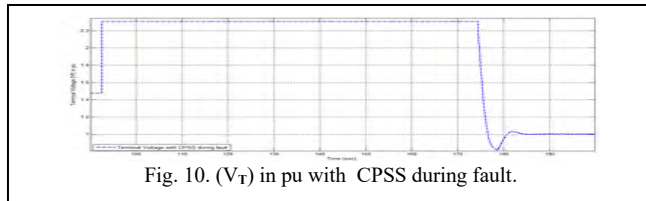


Fig. 10. (V_T) in pu with CPSS during fault.

observation: the parameter values remain the same with both the Conventional PSS (CPSS) and (PSS2B). This implies that the type of PSS used does not impact the power system's response during light load at the (PPGS). Consequently, the system's response is delayed in returning to stability, which manifests as a high settling time (t_s) value and a low damping ratio (ζ), as shown in Figures (6-9).

Therefore, to enhance the PSS's performance during light load faults, it is necessary to appropriately adjust the PSS2B's parameters and gain settings.

TABLE I. TERMINAL VOLTAGE (V_T) CHARACTERISTICS OF TRANSIENT CONDITIONS PARAMETERS (LIGHT LOAD).

parameters value	ON PSS	CPSS	PSS2B
damping ratio (ζ)	0.0788	0.0792	0.0781
maximum overshoot (%MP)	1.2817	1.2835	1.2789
un-damped natural frequency (ω_n) in sec	148.3908	148.3947	148.3529
Damped natural frequency (ω_d)	147.9299	147.9286	147.9003
peak time (t_p) in sec	0.0212	0.0212	0.0212
voltage terminal peak (V_{TP})	2.3050	2.3050	2.3050
settling time (t_s) in sec	0.000	185.137	180.764

TABLE II. ROTOR SPEED (ω_m) CHARACTERISTICS OF TRANSIENT CONDITIONS PARAMETERS (LIGHT LOAD).

parameters value	ON PSS	CPSS	PSS2B
damping ratio (ζ)	0.0000	0.3078	0.3076
maximum overshoot (%MP)	0.3621	0.3619	0.3622
un-damped natural frequency (ω_n) in sec	0.0247	0.0247	0.0247
Damped natural frequency (ω_d)	0.0235	0.0235	0.0235
peak time (t_p) in sec	133.7639	133.7647	133.7628
rotor speed peak (ω_{mp})	1.3620	1.3620	1.3621
settling time (t_s) in sec	158.363	158.359	158.412

TABLE III. ACTIVE POWER OUTPUT (P_{e0}) CHARACTERISTICS OF TRANSIENT CONDITIONS PARAMETERS (LIGHT LOAD).

parameters value	ON PSS	CPSS	PSS2B
damping ratio (ζ)	0.7668	0.7634	0.7616
maximum overshoot (%MP)	42.6431	40.9694	40.1185
un-damped natural frequency (ω_n) in sec	507.1499	503.987	502.3231
Damped natural frequency (ω_d)	325.5373	325.545	325.5411
peak time (t_p) in sec	0.0097	0.0097	0.0097
active power output peak (P_{e0})	6.1982	6.1983	6.1982
settling time (t_s) in sec	154.875	154.885	154.735

B. Transient state of PPGS during fault at normal load

Tables IV-VI present the transient parameter values which include damping ratio (ζ), maximum overshoot (%MP), undamped natural frequency (ω_n), damped natural frequency (ω_d), peak time (t_p), voltage terminal peak (V_{TP}), and settling time (t_s). These parameters are crucial in determining the response of Terminal voltage (V_T), Rotor speed (ω_m), and

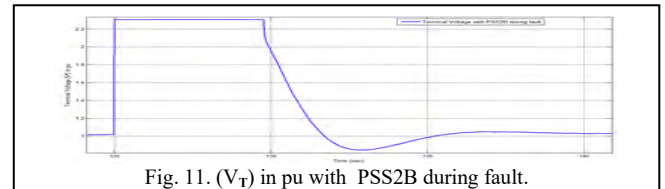


Fig. 11. (V_T) in pu with PSS2B during fault.

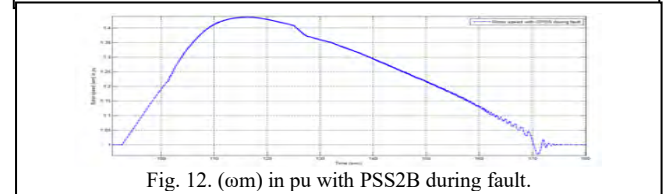


Fig. 12. (ω_m) in pu with PSS2B during fault.

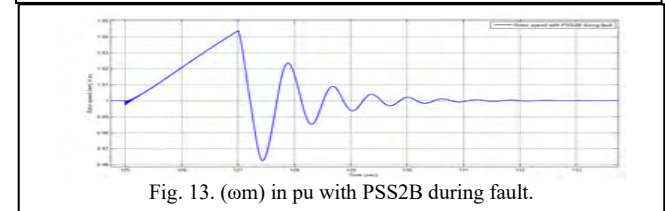


Fig. 13. (ω_m) in pu with PSS2B during fault.

Active power output (P_{e0}) with both conventional (PSS) and modern PSS (PSS2B). The results displayed in Tables IV-VI highlight that the use of PSS2B leads to improved values of damping ratio (ζ), maximum overshoot (%MP), and settling time (t_s) in comparison to the (CPSS). This indicates that the (PSS2B) significantly impacts the power system's response under normal operations at the (PPGS). As a result, the system response time is shorter, and the stability is achieved more quickly. This can be observed through the reduced settling time (t_s), and better values for damping ratio (ζ) and maximum overshoot, as shown in Figures 10-13.

TABLE IV. TERMINAL VOLTAGE (V_T) CHARACTERISTICS OF TRANSIENT CONDITIONS PARAMETERS (NORMAL LOAD).

parameters value	ON PSS	CPSS	PSS2B
damping ratio (ζ)	0.0826	0.0834	0.0330
Maximum overshoot (%MP)	1.2973	1.3007	1.1092

un-damped natural frequency (ω_n) in sec	197.6039	148.445	147.98
Damped natural frequency (ω_d)	197.6039	147.928	147.90
peak time (t_p) in sec	0.0212	0.0212	0.0212
voltage terminal peak (V_{TP})	2.3050	2.3050	2.305
settling time (t_s) in sec	197.604	199.97	133.94

TABLE V. ROTOR SPEED (ω_m) CHARACTERISTICS OF TRANSIENT CONDITIONS PARAMETERS (NORMAL LOAD).

parameters value	ON PSS	CPSS	PSS2B
damping ratio (ζ)	0.000	0.538	0.636
maximum overshoot (%MP)	0.438	0.438	0.423
un-damped natural frequency (ω_n) in sec	0.024	0.0243	0.222
Damped natural frequency (ω_d)	0.0235	0.0235	0.214
peak time (t_p) in sec	133.48	133.49	14.62
rotor speed peak (ω_{mp})	1.4384	1.4384	1.423
settling time (t_s) in sec	165.48	165.49	130.66

TABLE VI. ACTIVE POWER OUTPUT (P_{e0}) CHARACTERISTICS OF

parameters value	ON PSS	CPSS	PSS2B
damping ratio (ζ)	0.918	0.883	0.654
maximum overshoot (%MP)	1436.72	376.975	15.174
un-damped natural frequency (ω_n) in sec	820.694	695.635	430.602
Damped natural frequency (ω_d)	325.54	325.562	325.559
peak time (t_p) in sec	0.0097	0.0096	0.0096
active power output peak (P_{e0})	6.198	6.198	6.198
settling time (t_s) in sec	162.61	162.61	128.18

TRANSIENT CONDITIONS PARAMETERS (NORMAL LOAD).

C. Transient state of PPGS during fault at heavy load

Tables VII-IX show case the transient parameters' values, such as the damping ratio (ζ), maximum overshoot (%MP), undamped natural frequency (ω_n), damped natural frequency (ω_d), peak time (t_p), voltage terminal peak (V_{TP}), and settling time (t_s). These parameters dictate the response of Terminal voltage (V_T), Rotor speed (ω_m), and Active power output (P_{e0}) under the conventional (PSS) and modern PSS (PSS2B). The results from Tables VII-IX reveal that when PSS2B is applied, the system exhibits favorable values for damping ratio (ζ), maximum overshoot (%MP), and settling time (t_s) compared to (CPSS). This implies that (PSS2B) positively influences the power system response under heavy load at the PPGS. Consequently, the system response time is reduced, allowing for quicker stabilization, as evidenced by the shorter settling time (t_s) shown in Figures (14-17).

TABLE VII. TERMINAL VOLTAGE (V_T) CHARACTERISTICS OF TRANSIENT CONDITIONS PARAMETERS (HEAVY LOAD).

parameters value	ON PSS	CPSS	PSS2B
damping ratio (ζ)	0.0829	0.082	0.038
Maximum overshoot (%MP)	1.2986	1.298	0.884
un-damped natural frequency (ω_n) in sec	148.44	148.44	148.013

Damped natural frequency (ω_d)	147.92	147.929	147.901
peak time (t_p) in sec	0.021	0.0212	0.021
voltage terminal peak (V_{TP})	2.305	2.305	2.305
settling time (t_s) in sec	249.76	249.867	137.46

TABLE VIII. ROTOR SPEED (ω_m) CHARACTERISTICS OF TRANSIENT CONDITIONS PARAMETERS (HEAVY LOAD).

parameters value	ON PSS	CPSS	PSS2B
damping ratio (ζ)	0.0000	0.2079	0.2568
maximum overshoot (%MP)	0.5128	0.5128	0.4340
un-damped natural frequency (ω_n) in sec	0.0241	0.0241	0.2332
Damped natural frequency (ω_d)	0.0235	0.0235	0.2254
peak time (t_p) in sec	133.4175	133.4184	13.9366
rotor speed peak (ω_{mp})	1.5128	1.5128	1.4341
settling time (t_s) in sec	174.084	174.522	131.757

TABLE IX. ACTIVE POWER OUTPUT (P_{e0}) CHARACTERISTICS OF TRANSIENT CONDITIONS PARAMETERS (HEAVY LOAD).

parameters value	ON PSS	CPSS	PSS2B
damping ratio (ζ)	0.8837	0.9421	0.5960
maximum overshoot (%MP)	376.2062	6817.7343	10.2941
un-damped natural frequency (ω_n) in sec	695.4802	971.0196	405.4409
Damped natural frequency (ω_d)	325.5773	325.5773	325.5733
peak time (t_p) in sec	0.0096	0.0096	0.0096
active power output peak (P_{e0})	6.1983	6.1983	6.1983
settling time (t_s) in sec	171.857	171.142	129.484

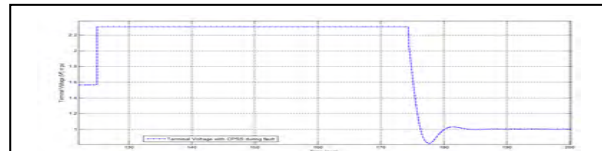


Fig. 14. (V_T) in pu with CPSS during fault.

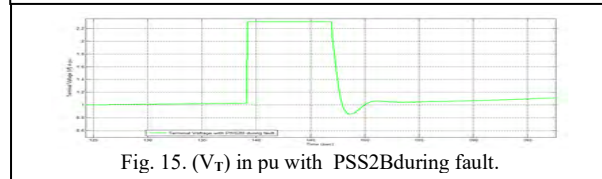


Fig. 15. (V_T) in pu with PSS2B during fault.

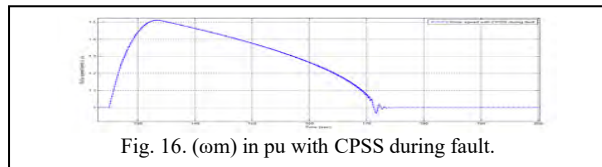


Fig. 16. (ω_m) in pu with CPSS during fault.

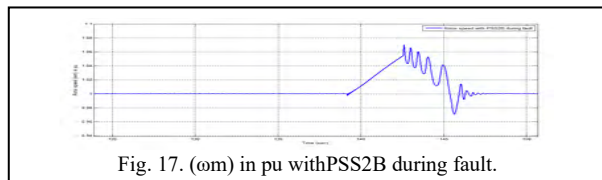


Fig. 17. (ω_m) in pu with PSS2B during fault.

V. CONCLUSION

An empirical investigation conducted at the Peerdawod Gas Power Station provided valuable observations on the behavior of transient state conditions during a three-phase

fault that persisted for a duration of 2 seconds. The Power System Stabilizer (PSS2B) demonstrated remarkable performance compared to the conventional PSS (CPSS). The (PSS2B), which has two inputs - active power (P_{e0}) and rotor speed deviation ($d\omega$), outperformed the (CPSS), which only has a single input, (P_{e0}). Nevertheless, it is acknowledged that although (PSS) is essential in mitigating high disturbances, it can have adverse effects during steady-state conditions, normal load fluctuations, and initial transient periods. In such cases, relying solely on the excitation control system is usually sufficient. The study also found a notable correlation between the load type and the performance of the (PSS) in transient states. More precisely, when dealing with high loads that have a power factor (P.F) of 95%, (PSS2B) caused excessive voltage after a fault occurred, along with unfavorable values of damping ratio (ζ) and maximum overshoot. Under conditions of low electrical demand and a power factor of 60%, voltage fluctuations were observed during faults, resulting in a prolonged recovery time and the possibility of a system failure. The power system stabilizer (PSS) had limited impact in mitigating these issues. In contrast, (PSS2B) demonstrated outstanding performance under typical loads, characterized by a power factor of (75% - 80%). It effectively restored system stability during intense fault conditions, promptly preventing system collapse by optimizing the damping ratio (ζ), minimizing overshoot, and reducing settling time. The Peerdawod Gas Power Station (PPGS) configures the PSS parameters to be suitable for normal loads (PF of 75% - 80%) in the event of high disturbance faults. The significance of employing an intelligent algorithm to select the optimal (PSS) parameter values, taking into account load fluctuations, was emphasized. It is essential to adjust the PSS parameters, taking into consideration the load type and other pertinent factors within the power system. The parameter values (T1, T2, T3, T4, T10, T11) of (PSS2B) at (PPGS) are specifically tailored for typical load conditions (PF 75% - 80%) during significant disturbances caused by faults. Nevertheless, the (PSS2B) does not operate when the load is light, causing the system to consume a greater amount of reactive power before and during faults. This highlights the necessity of adjusting these parameters according to the current conditions of the power system. Ultimately, the study emphasizes the significance of selecting the suitable PSS configuration, considering fluctuations in load, and adjusting the parameters accordingly. These factors are crucial for guaranteeing the best possible performance and stability of the system, as demonstrated by the situation at the Peerdawod Gas Power Station. Therefore in the future work must be tuning the parameter values (T1, T2, T3, T4, T10, T11) of (PSS2B) at (PPGS) using evaluation techniques such as Genetic Algorithms (GA) to optimizing these parameters during all load cases to improving the performance of the (PSS2B) and to make the power system more stable when the fault occurs.

ACKNOWLEDGMENT

We extend our sincere gratitude to the Electrical Engineering Team at Peerdawod Power Station in Erbil-KRD for their invaluable assistance and unwavering support

throughout our research period at the station. Their dedication, cooperation, and willingness to share their expertise were instrumental in the success of our work. We are particularly grateful for their prompt responses to our inquiries and insightful advice, which significantly enhanced our understanding of the station's .

REFERENCES

- [1] Nader M.A. Ibrahim, Basem E. Elnaghi, Hamed A. Ibrahim, and Hossam E.A. Talaat, "Modified Particle Swarm Optimization Based on Lead-Lag Power System Stabilizer for Improve Stability in Multi-Machine Power System," *International Journal on Electrical Engineering and Informatics* , vol. 11, no. 1, pp. 161-182, March 2019.
- [2] Abdelhay A. Sallam and Om P. Malik, *Power System Stability Modelling, analysis and control*, The Institution of Engineering and Technology, 1st Edition, ch. 1, pp. 1-10 , sec. 3, ch. pp. 145-218, 2015.
- [3] Dr. Farid Golnaraghi, Dr. Benjamin C. Kuo, *Automatic Control Systems*, McGraw-Hill Education, 10th Edition, ch. 1, ch. 5, 2017.
- [4] Leonard L. Grigsby, *Power System Stability and Control*, 3rd Edition, sec. 2, ch. 8, ch. 13, pp. 1-10, 2012.
- [5] N. Hatziaargyriou et al., "Definition and Classification of Power System Stability – Revisited & Extended," in *IEEE Transactions on Power Systems*, vol. 36, no. 4, pp. 3271-3281, July 2021, doi: 10.1109/TPWRS.2020.3041774.
- [6] G. M. Giannuzzi, V. Mostova, C. Pisani, S. Tessitore, and A. Vaccaro, "Enabling Technologies for Enhancing Power System Stability in the Presence of Converter-Interfaced Generators," *Energies*, vol. 15, no. 21, p. 8064, Oct. 2022, doi: 10.3390/en15218064.
- [7] E. S. Bayu, B. Khan, Z. M. Ali, Z. M. Alaas, and O. P. Mahela, "Mitigation of Low-Frequency Oscillation in Power Systems through Optimal Design of Power System Stabilizer Employing ALO," *Energies*, vol. 15, no. 10, p. 3809, May 2022, doi: 10.3390/en15103809.
- [8] N. Hatziaargyriou et al., "Definition and Classification of Power System Stability – Revisited & Extended," in *IEEE Transactions on Power Systems*, vol. 36, no. 4, pp. 3271-3281, July 2021, doi: 10.1109/TPWRS.2020.3041774.
- [9] T. S. Borsche, T. Liu and D. J. Hill, "Effects of rotational Inertia on power system damping and frequency transients," 2015 54th IEEE Conference on Decision and Control (CDC), Osaka, Japan, 2015, pp. 5940-5946.
- [10] Norman S. Nise ,*Control Systems Engineering*, John Wiley & Sons, Inc, 6th Edition, ch. 4, pp. 169-232, 2015.
- [11] Dr. Farid Golnaraghi, Dr. Benjamin C. Kuo, *Automatic Control Systems*, McGraw-Hill Education, 10th Edition, ch.7, 2017.
- [12] Y. A. Sha'aban, "The Effect of Dead-Time and Damping Ratio on the Relative Performance of MPC and PID on Second Order Systems," *Applied Sciences*, vol. 13, no. 2, p. 1138, Jan. 2023, doi: 10.3390/app13021138.
- [13] Debasis Acharya, Dushmanta Kumar Das, and Ankur Rai, "Particle Swarm Optimization (PSO) based 2-DoF-PID power system stabilizer design for damping out low frequency oscillations in power systems", 2019 2nd International

- Conference on Innovations in Electronics, Signal Processing and Communication (IESC), IEEE, pp. 148–153, Shillong, India, 18 November 2019.
- [14] M. Mahdavian, G. Shahgholian, M. Janghorbani, S. Farazpey and M. Azadeh, "Analysis and simulation of PID-PSS design for power system stability improvement," 2016 13th International Conference on Electrical Engineering/Electronics, Computer, Telecommunications and Information Technology (ECTI-CON), Chiang Mai, Thailand, 2016, pp. 1-6.
- [15] X. Xiong, C. Wu, B. Hu, D. Pan and F. Blaabjerg, "Transient Damping Method for Improving the Synchronization Stability of Virtual Synchronous Generators," in *IEEE Transactions on Power Electronics*, vol. 36, no. 7, pp. 7820-7831, July 2021.
- [16] Prabha S Kundur, Om P Malik, *Power System Stability and Control*, Second Edition, McGraw-Hill Education, 2022, ch 8. sec. 2, pp. 255–265.
- [17] Jawaharlal Bhukya, Vasundhara Mahajan, "Mathematical modelling and stability analysis of PSS for damping LFOs of wind powersystem," *IET Renew, Power Gener.*, Vol. 13, Iss. 1, pp. 103-115, 2019.
- [18] Hoon-Gi Lee, Jun-Ho Huh, "A Cost-Effective Redundant Digital Excitation Control System and Test Bed Experiment for Safe Power Supply for Process Industry 4.0," *MDPI*, vol. 6, no. 7, pp.1-29, July 2018.
- [19] G. Xu, Z. Wang, W. Li, Y. Zhan, H. Zhao and Y. Luo, "Study on Power Tracking Excitation Control and Parameters Sensitivity of Dual-Excited Synchronous Generator," 2021 IEEE Energy Conversion Congress and Exposition (ECCE), Vancouver, BC, Canada, 2021, pp. 4240-4245.
- [20] Joe H. Chow; Juan J. Sanchez-Gasca, "Excitation Systems," in *Power System Modeling, Computation, and Control*, IEEE, 2020, pp.237-263.
- [21] Jerkovic, Vedrana; Miklosevic, Kresimir; Spoljaric Zeljko, "Excitation System Models of Synchronous Generator," 28 th International Conference Science in Practice, September 2018.
- [22] Abdelhay A. Sallam and Om P. Malik, *Power System Stability: Modelling, Analysis and Control*, 1st Edition, Institution of Engineering and Technology, London, United Kingdom, ch. 11, sec. 4, pp. 277-300, 2015.
- [23] Gowrishankar Kasilingam and Jagadeesh Pasupuleti, "Coordination of PSS and PID Controller for Power System Stability Enhancement – Overview," *Indian Journal of Science and Technology*, Vol. 8, Iss. 2, pp. 141-151, 2015.
- [24] Vijaya Lakshmi A.S.V, Ramalinga Raju Manyala, and Siva Kumar Mangipudi, "Design of a robust PID-PSS for an uncertain power system with simplified stability conditions", *Protection and Control of Modern Power Systems*, vol. 20, no. 5, pp. 1-6, 29 September 2020.
- [25] Azade Abedini, Ghazanfar Shahgholian, and Bahdor Fani, "Power System Dynamic Stability Improvement Using PSS Equipped with Microcontroller," *International Journal of Smart Electrical Engineering*, Vol.10, No.2, pp. 67-76, Spring 2021, doi: 10.30495/ijsee.2021.683681.
- [26] M.S. Shahriar M. Shafiullah, M.I.H. Pathan, Y.A. Sha'aban, Housseem R.E.H. Boucekara, Makbul A.M. Ramli, M.M. Rahman, "Stability improvement of the PSS-connected power system network with ensemble machine learning tool," *Energy Reports*, vol. 8, pp. 11122–11138, 9 September 2022.
- [27] F. D. Marco, P. Rullo and N. Martins, "Synthetic Power System Models for PSS Tuning and Performance Assessment," 2021 IEEE Electrical Power and Energy Conference (EPEC), Toronto, ON, Canada, 2021, pp. 107-112.
- [28] A. MOSHREF, H. TAGOURTI, N. WOOSTER, R. HARRISON, and T. RICIO PPO, "Power System Stabilizer Tuning with Presence of Torsional Oscillations," 2019 CIGRE Canada Conference, vol. 111, pp. 1–8, Montréal, Québec, September, 2019.
- [29] Fan Mengjing, Wang Kewen, and Zhang Jianfen, "Parameters Setting of power system stabilizer PSS2B," in 2016 4th International Conference on Renewable Energy and Environmental Technology (ICREET), 2016, vol. 112, pp. 1–8, doi: 10.2991/icreet-16.2017.12.
- [30] M.S. Shahriar M. Shafiullah, M.I.H. Pathan, Y.A. Sha'aban, Housseem R.E.H. Boucekara, Makbul A.M. Ramli, M.M. Rahman, "Stability improvement of the PSS-connected power system network with ensemble machine learning tool," *Energy Reports*, vol. 8, pp. 11122–11138, 9 September 2022.
- [31] Ali, O. M. A., Kareem, S. W., & Mohammed, A. S. (2022, February). Evaluation of electrocardiogram signals classification using CNN, SVM, and LSTM algorithm: A review. In 2022 8th International Engineering Conference on Sustainable Technology and Development (IEC) (pp. 185-191). IEEE.
- [32] Ma, R., Kareem, S. W., Kalra, A., Doewes, R. I., Kumar, P., & Miah, S. (2022). Optimization of electric automation control model based on artificial intelligence algorithm. *Wireless Communications and Mobile Computing*, 2022.